

1 **Historical reconstruction of small-scale gold mining impact in tropical**
2 **wetland sediments Bajo Cauca-Antioquia, Colombia.**

3 **Diana María Agudelo-Echavarría¹, Carolina Olid², Francisco Molina-Pérez¹,**
4 **Pedro Pablo Vallejo-Toro¹, Jordi Garcia-Orellana^{3,4}.**

5 ¹ Grupo de Investigación en gestión y modelación ambiental (GAIA), Escuela
6 Ambiental, Facultad de Ingeniería, *Universidad de Antioquia UdeA*, Calle 70 No.
7 52-2, Medellín, Colombia, diana.agudelo@gmail.com.

8 ² Climate Impacts Research Centre (CIRC). Dept. of Ecology and Environmental
9 Science, Umeå University, Sweden

10 ³ Departament de Física, Facultat de Ciències, Universitat Autònoma de
11 Barcelona, Spain

12 ⁴ Institut de Ciència i Tecnologia Ambientals (ICTA), Universitat Autònoma de
13 Barcelona, Spain

14 **Abstract**

15 Global mining investment in Latin America has increased exponentially over the
16 last decade, resulting in the release of vast amounts of toxic metals into the
17 environment. Here, historical trends of trace metals (i.e., Hg, Cr, Cu, Ni and Pb) of
18 small-scale Gold Mining (ASGM) were reconstructed using a dated (²¹⁰Pb and
19 ¹³⁷Cs) sediment core collected from a tropical wetland located in Antioquia
20 (Colombia), a region characterized by increased mining development over the past
21 century. Results showed that metal concentrations at the beginning of the 20th
22 century were similar to background values, indicating that there is no impact of any
23 previous anthropogenic activities. The significant increase in both sediment
24 accumulation rates and total organic carbon (TOC) that occurred in the 1940s

25 reflects the deforestation of the area due to the diversification of the economy (e.g.
26 coffee cultivation, mining or animal husbandry). Both concentrations and
27 accumulation rates of metals increased exponentially after the 1980s due to the
28 reactivation of alluvial gold exploitation, reaching concentrations that exceeded up
29 to 2-5 times the background values.

30 **Keywords:** *gold Mining, heavy metals, contamination, ²¹⁰Pb dating, tropical*
31 *wetland*

32 **1. Introduction**

33 Artisanal and Small-scale Gold Mining (ASGM) is one of the main activities that
34 introduces vast amount of heavy metals (e.g. Ag, Cr, Cu, Hg, Ni, Pb, Zn) into the
35 environment (Adriano, 2001; Lar et al., 2015; Camizuli et a. 2018; Aliyu et al.,
36 2018). Although mining activities provide large economic benefits for companies
37 and governments, high amounts of metals introduced into the biosphere may have
38 adverse effects on human and environmental health (Singh and Kalamdhad, 2011;
39 Niane et al., 2014; Hilson, 2016; Gerson et al., 2018). According to the United
40 Nations Environment Programme - UNEP (2018), the ASGM sector contributes for
41 approximately 15% of total global Hg emissions and accounts for up to 80% of the
42 metal emissions from South America and Sub-Saharan Africa. Surprisingly,
43 activities such as ASGM are still not regulated in more than 70 countries (WHO,
44 2013).

45 Although mercury (Hg) is often the focus of studies investigating ASGM (Silva-Filho
46 et al., 2006; Grimaldi et al., 2008; Balzino et al., 2015; Diringer et al., 2015; Mora
47 et. al., 2018), there are other heavy metals released during these activities such as
48 silver (Ag), chromium (Cr), copper (Cu), nickel (Ni), lead (Pb) and zinc (Zn). The

49 combination of their toxicity and the resulting loss of biodiversity has led to
50 dramatic consequences for human population, such as migration due to the
51 destruction of subsistence resources as well as the development of endemic
52 diseases (Palacios-Torres et. al., 2018, Betancur-Corredor et. al., 2018). This
53 increases the conflict between economically profitable ventures and natural
54 ecosystems (Kahhat et al., 2019). An example of this conflict is Colombia, where
55 ASGM constitutes about 2% of Gross Domestic Product GDP (Güiza and
56 Aristizabal, 2013) and plays an important role in the national economy. In 2010, the
57 ASGM sector in Colombia had 200000 miners officially producing 30 t of gold per
58 year. In the administrative department of Antioquia, there were 17 mining towns
59 (including Nechí municipality) and about 15% artisanal gold miners all over the
60 country. This intensive mining activity positioned the Department of Antioquia as
61 the world's largest mercury polluter per capita from ASGM (Cordy et al., 2011). By
62 the 2013, after a substantial effort of the government, annual mercury releases into
63 the environment were reduced by 63%, resulting in 46 to 70 tons (García et al.,
64 2015). The amount of metals released and their impacts were greatest for nearby
65 aquatic systems (lakes, streams or rivers) and wetlands due to the need for access
66 to water (Ho et al., 2010; Rungwa et al., 2013, Manoj et. al., 2018). Other activities,
67 such as intensive livestock farming and agriculture, also contribute to the increase
68 in metal concentrations in aquatic systems in the region (Marrugo-Negrete et al.,
69 2017).

70 During ASGM activities rocks and ore are first crushed into small pieces by hand
71 that is then added with water into motorized mills. Because water is used, ASGM
72 facilities are often built near waterways such as rivers, which can later be subject to

73 severe metal pollution. The impact of ASGM in the environment can be monitored
74 checking the quality of suspended particles in rivers and streams (Ji et al. 2016;
75 Lartiges et al. 2001). However, to integrate changes in the quality of the particles
76 over long time periods river sediments as environmental archive is often more
77 useful. However, the temporal metal trends in fluvial sediments are frequently
78 punctuated by higher-order fluctuations related to geomorphologic control of fluvial
79 sedimentation, grain size, hydrological factors and short-term redistribution events
80 such as floods (Herr and Gray, 1996; Nguyen et al., 2009; Bábek et al., 2011).
81 Therefore, the historical reconstruction of metal fluctuations make the interpretation
82 of past contamination flowing through river a difficult task.

83 Wetlands are considered as sinks for a wide range of chemical compounds,
84 because of the presence of fine grain sediments and high organic matter content
85 that increases the influence on the cation exchange capacity and therefore, the
86 retention of those contaminants (Devesa-Rey et al., 2011; Gu et al., 2015; Kang et
87 al., 2017). Sediment records collected in wetlands are commonly used to study the
88 quality of these ecosystems (Gan et al., 2013; Chen et al., 2016; Zhu et al., 2019),
89 as they allow to quantify the degree of pollution or contamination of the system.
90 Pollution occurs when there is damage to organisms and the ecosystem.
91 Contamination is defined as the presence of a chemical above natural
92 concentrations in the area; however, this concentration does not cause damage
93 (Chapman, 2007). Moreover, the use of dated sediment records is a common way
94 of providing important information on past environmental changes in aquatic
95 ecosystems, especially in situations where there is lack of past data (Puig and

96 Palanques, 1998; Garcia-Orellana et al., 2011). To this purpose, the natural
97 radionuclide ^{210}Pb ($T_{1/2} = 22.3$ years) is often used to establish the chronology of
98 recent sedimentary records accumulated over the past 100-150 years (Appleby
99 and Oldfield, 1992), period when the most dramatic changes due to anthropogenic
100 activities have occurred in the environment. Because anthropogenic, physical or
101 biological processes could alter the ^{210}Pb record, the ^{210}Pb -derived chronology
102 should be verified with other dating tracers such as artificial radionuclides (^{90}Sr ,
103 ^{137}Cs , $^{239,240}\text{Pu}$ and ^{241}Am) (Smith, 2001; Sang-Han et al., 2005) that were
104 introduced in the environment during the nuclear weapons testing in the 50-60s
105 and later, and mainly in Europe, during the 80s due to the Chernobyl accident.

106 Several studies carried out in lakes in Colombia provided accurate estimations of
107 the impact of ASGM activities in South America (Telmer and Veiga, 2009; Adler et.
108 al, 2013; Moreno-Brush et. al., 2016; Adler et. al, 2017; Marshall et. al., 2018). But
109 some other sediment reservoirs in highly impacted areas such as wetlands, have
110 not yet been widely studied over time, making it difficult to estimate the regional
111 impact of mining activities in tropical zones. A study conducted by the United
112 Nations Office on Drugs and Crime in 2018 determined that out of the 83,620 ha
113 with gold mining operation identified in 2016 in Colombia, more than 30,900 ha
114 were part of the territory of Antioquia (37% of the total Colombia territory). Thus,
115 this area contributed to the 41% of the Colombia national gold production
116 (UNODC, 2018). However, there are not studies that have determined
117 accumulation of heavy metals in Antioquia to assess the current impact of ASGM.
118 With this objective, we reconstructed recent (past 100-150 years) historical trends
119 in both concentrations and accumulation rates of trace metals (Cr, Cu, Hg, Ni, Pb,

120 and Zn) using a wetland sediment core. Thus, comparing metals concentrations,
121 released by anthropogenic activities, with background values helped us to evaluate
122 the historical impact of ASGM on nearby wetland ecosystems.

123 **2. Materials and methods**

124 **2.1 Study area**

125 Las Palmas wetland is located in the district of La Concha – Nechí (7°07'53.69" -
126 8°01'45.87" N and 74°54'46.20" - 74°47'45.43" W), region of Bajo Cauca,
127 department of Antioquia (Colombia) (Figure 1). The region has a tropical climate,
128 with annual temperatures and precipitation ranging between 28 and 30 °C and
129 from 2000 to 4000 mm, respectively. The dry season is from January to March and
130 from July to September, while the rainy season is from October to December and
131 from April to June (Betancur et al., 2009, OECD, 2016).

132 Las Palmas wetland is located on the left margin of the Nechí River, which is the
133 most important tributary of the Cauca River. The wetland is located within two
134 geological formations: the alluvial deposits of the Nechí River and the Caucasia
135 Formation, which is of a great economic importance for its gold reserves (Zapata et
136 al., 2013). Geomorphological units in the wetlands include floodplains, flooded
137 lowlands, and partially flooded high plains with a low undulating topography
138 between 30 and 600 m above sea level. Lateral erosion by scouring affects the
139 margin of the rivers in some stretches. The high biodiversity and natural resources
140 (e.g. wood and minerals) of Las Palmas is currently threatened by anthropogenic
141 activities such as mining and agriculture (Alcaldía Municipal de Nechí, 2000).

142 The most important gold deposits in Colombia are located in three regions. One of
143 them is the drainage basin of the Cauca River that belongs to Las Palmas wetland

144 (Acemoglu et al., 2012). Las Palmas is one of the areas with the highest mining
145 exploitation in the Bajo Cauca Antioqueño, and represents one of the main
146 wetlands of the riverine complex. Moreover, the department of Antioquia has
147 yielded the most significant gold outputs over the last 10 years, with around 40% of
148 the total national production (Betancur-Corredor et al., 2018). Thus, studying this
149 area is essential to understand the impacts that mining activity have and still cause
150 to the wetland ecosystems.

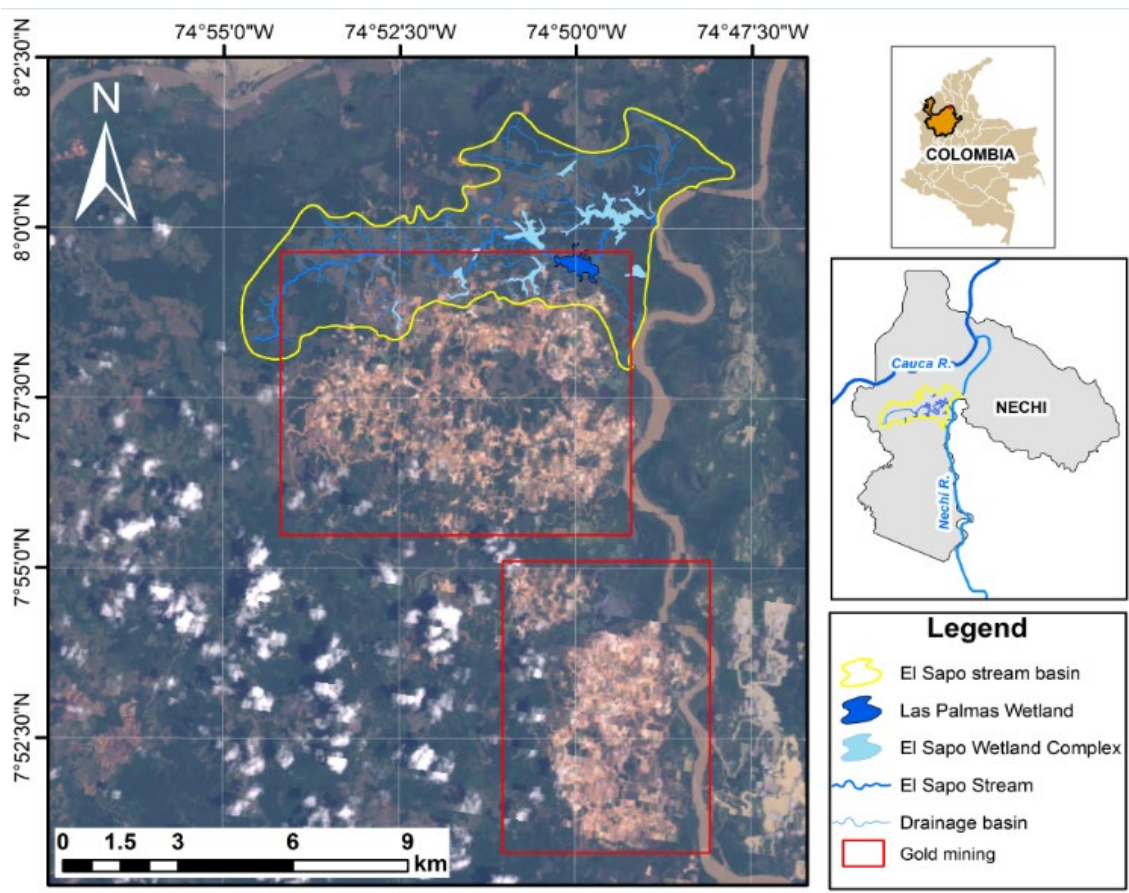


Figure 1. Location of Las Palmas wetland (Antioquia department, Colombia)

151 **2.2 Sampling**

152 Due to that the objective of a radiochronology is to describe the temporal
153 evolution of the contamination recorded due to anthropogenic activities as

154 accurately as possible, the information contained in one core is intrinsically valid,
155 since it represents the evolution of this part of the ecosystem over time (Sanchez-
156 Cabeza et al., 2012). Core sampling was based on the criteria established for the
157 sampling of sediment cores provided in Sanchez-Cabeza et al. (2012), where the
158 fundamental objective is to obtain an unaltered sediment record, avoiding the
159 mixing of the strata, and thus guaranteeing the adequate resolution of
160 environmental changes. The center of Las Palmas complied with the conditions
161 defined above, since this was the area that had the least influence of the
162 tributaries of the wetland (Río Nechí and Quebrada El Sapo) and the
163 anthropogenic activities that take place in the wetland area of influence.

164 A sediment core (6.6 cm diameter, 371 cm length) was collected in 2014 from the
165 center of Las Palmas wetland during the rainy season using a Livingstone/Bolivia
166 corer following the procedure outlined by the Limnological Research Center
167 (<http://lrc.geo.umn.edu/lacore/assets/pdf/sops/livingstone-bolivia.pdf>).

168 Sampling was carried out in the rainy season (November) due to difficult access
169 to the area during the dry season, when channels of access to the wetland dry up
170 and impedes access to the area. Once collected, the core was transported to the
171 laboratory and stored at 4 °C until further analysis. The core was sliced every 1
172 cm following the procedures established by Loring and Rantala (1992). Samples
173 were weighed before and after freeze drying to determine water content and bulk
174 density. Subsamples of each section were ground using an agate mortar and
175 stored in polyethylene bags for further analysis.

176 **2.3 Laboratory analysis**

177 Intact samples were analyzed for grain size following a standard laser diffraction

178 method (ISO, 2009) and using a particle size analyzer (Beckman Coulter LS 230)
179 after an oxidative treatment with H₂O₂ (10%). For the analysis of total organic
180 carbon (TOC), approximately 0.3 g ground sediment samples were oxidized with
181 a mixture of K₂Cr₂O₇ and H₂SO₄ (2.5:3.75 mL, respectively) in a hot plate (120 °C,
182 60 min). TOC content was determined using a spectrophotometer UV/VIS (Merck
183 Pharo 300) (ISO, 1998). Precision was evaluated by measuring the values of
184 relative standard deviation (RSD) of a set of data. The RSD values obtained for
185 repeatability tests was 2.92% and recovery was evaluated through six replicates
186 of the certified reference material NIST SRM-1944- New York/New Jersey
187 Waterway Sediment and the resulting was 92.9%.

188 Metals analysis (Al, Cr, Cu, Ni, Pb and Zn) was carried out by atomic absorption
189 spectrophotometry (Thermo Scientific AA iCE3300). Mercury (Hg) content was
190 analyzed by cold vapor generation technique (Buck 410) after acid digestion
191 (HNO₃ + HCl + HF, 5:4:1 mL) of dried sediment samples in closed Teflon PFA
192 containers on a microwave oven (700 W, 70 s). The limit of quantitation (LoQ)
193 values found were of 0.750 mg L⁻¹, 0.1 mg L⁻¹, 0.010 mg L⁻¹, 0.020 mg L⁻¹, 0.050
194 mg L⁻¹, 0.047 mg L⁻¹ and 0.025 µg for Al, Cr, Cu, Ni, Pb, Zn and Hg respectively.
195 Precision was evaluated by measuring the values of relative standard deviation
196 (RSD) of a set of data. RSD values obtained for repeatability tests were 3.10% (Al),
197 6.22% (Cr), 8.21% (Cu), 13.76% (Ni), 13.55% (Pb), 12,39% (Zn) and 12.62% (Hg).
198 The recovery study was carried out by spiking technique. Known concentration of
199 standard solutions (Al, Cr,Cu, Ni, Pb, Zn and Hg) were added to certified reference
200 material - IAEA SL-1 (Trace and Minor Elements in Lake Sediment), and the
201 resulting spiked samples compared to the known value of standard solutions

202 added. The average recovery values were $104 \pm 3\%$ (Al), $95 \pm 7\%$ (Cr), $102 \pm 2\%$
203 (Cu), $101 \pm 2\%$ (Ni), $100 \pm 2\%$ (Pb), $105 \pm 2\%$ (Zn) and $100 \pm 5\%$ (Hg). Total
204 activities of ^{210}Pb were estimated by alpha spectrometry through its daughter
205 product ^{210}Po , assumed in secular equilibrium with ^{210}Pb (Flynn, 1968; Hamilton
206 and Smith, 1986, Sanchez-Cabeza et al. 1998). Briefly, sediment samples were
207 acid digested with HF and HNO_3 (3:9 mL) after spiking with a known amount of
208 ^{209}Po yield tracer. After this, Po isotopes were plated onto silver disks immersed
209 into a solution of HCl (1M) for 6 hours. To ensure the analytical quality of the
210 process and to assess the reproducibility of the results, a replicate was prepared
211 for each group of samples. Recovery of the method was evaluated by measuring a
212 certified sediment reference material IAEA-315 ($103 \pm 4\%$). Discs were measured
213 using Passive Implanted Planar Silicon (PIPS) (CANBERRA, model PD-450.18
214 A.M.) and silicon surface barrier (EG&G Ortec Mod. SSB 450R) alpha
215 spectrometers. Discs were measured until achieving less than 5% of uncertainty in
216 the ^{210}Po counting rate or a maximum counting time of 400,000 s. In order to
217 constrain the age model and to determine the supported ^{210}Pb from ^{226}Ra , some
218 samples were analyzed by gamma spectrometry. Thus, activities of ^{137}Cs and
219 ^{226}Ra were measured by using a calibrated geometry high-resolution, high-purity
220 germanium (HPGe) detector (Canberra) for 2 - 3 days. Dried and grained samples
221 were sealed and stored for three weeks before counting to ensure secular
222 equilibrium between ^{226}Ra daughters. ^{137}Cs was quantified via its γ -emission at 662
223 keV (MDA= 3 - 8 Bq kg^{-1}) and ^{226}Ra via the γ -emission at 351 keV (MDA= 6 - 12 Bq
224 kg^{-1}) of its daughter nuclide ^{214}Pb .

225 **2.4 Sediment chronology**

226 Sediment core chronology was determined by applying the Constant Rate of
227 Supply (CRS) model (Appleby and Oldfield, 2001). This model assumes a constant
228 flux of ^{210}Pb (excess $^{210}\text{Pb} - ^{210}\text{Pb}_{\text{xs}}$, derived from subtracting the supported ^{210}Pb
229 from the total ^{210}Pb) to the sediment and allows the rate of sedimentation to vary
230 over time. The CRS model also provides estimation of both mass accumulation
231 rates (MAR, $\text{g m}^{-2} \text{y}^{-1}$) and sediment accumulation rates (SAR, cm y^{-1}).

232 **2.5 Statistical analysis**

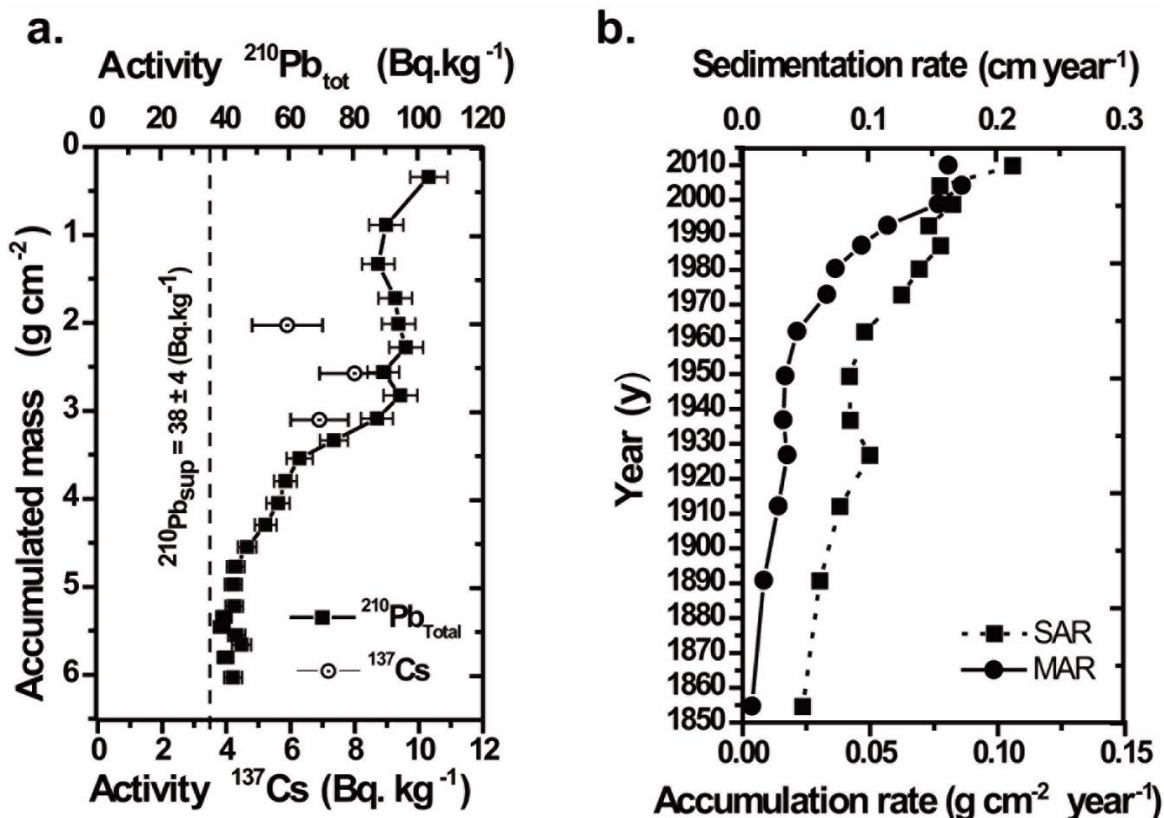
233 A correlation analysis was applied on the entire data set (grain size, TOC, mass
234 accumulation rates and metal concentrations) using raw or normalized metal
235 concentrations according to the degree of correlation with Al content. In order to
236 understand the processes that control metal distribution in the wetland, the
237 distribution of the selected elements was studied using a principal component
238 analysis (PCA) Logarithmic transformation and data standardization were carried
239 out to carry (Reimann et. al., 2002; Rencher, 2002). Here, the Spearman
240 correlation matrix to compensate the differences in the scale of the values between
241 variables was analyzed. The analysis was carried out using R-version 3.5.3: R
242 (Core Team, 2018).

243 **3. Results and discussion**

244 **3.1 Sediment chronology and sedimentation rates**

245 ^{210}Pb activities decreased exponentially with depth (Figure 2a). However, an
246 almost constant ^{210}Pb activity (mean of $92 \pm 3 \text{ Bq kg}^{-1}$) was observed between 0.9
247 and 2.8 g cm^{-2} (between 2 and 8 cm). Considering the assumptions stated by the

248 CRS model, this constant activity in ^{210}Pb is ascribed to an increase in mass
249 accumulation rate. This increase in sediment accumulation rates is consistent with
250 the metal concentration profiles that showed a similar pattern in the same sections
251 (see section 4.2). This type of ^{210}Pb distribution can also be obtained by physical
252 and biological mixing. However, the application of the CRS in these altered ^{210}Pb
253 profiles would introduce a deviation from the real age up to only 4%, which is of the
254 same order that the uncertainty associated to the age-depth model (Arias-Ortiz et
255 al., 2018). Thus, the CRS model seems to be the most suitable model to derive
256 consistent chronologies for our core. At the bottom of the profile, ^{210}Pb activities
257 were almost constant and similar to the mean measured activity of ^{226}Ra (35 ± 4
258 Bq kg^{-1}). This constant value was taken as representative of the supported ^{210}Pb
259 and subtracted from the total ^{210}Pb activities to obtain the excess ^{210}Pb fraction,
260 used for dating. The CRS model was applied to the unsupported ^{210}Pb distribution,
261 and an age of 159 ± 24 years was obtained for the upper 4.5 g cm^{-2} (15 cm) of
262 accumulation.



263

264 **Figure 2.** a) Total ^{210}Pb and ^{137}Cs concentration profile and b) Mass Accumulation
 265 Rates (MAR) and Sedimentation Rates (SR) in Las Palmas wetland sediment core.
 266 Activities of ^{137}Cs were detected between 2.0 and 3.1 g cm^{-2} , with concentrations
 267 ranging from 5.9 and 8.0 Bq kg^{-1} (Figure 2a). A peak of ^{137}Cs , corresponding to the
 268 year 1973 \pm 2, can be inferred, which is in good agreement with the historical
 269 deposition of ^{137}Cs in the south hemisphere (Pennington et al., 1973). The deepest
 270 layer with detectable ^{137}Cs activity was located in 1950 \pm 4, also consistent with the
 271 beginning of the global fallout period (1954). The consistency of the temporal
 272 changes of ^{137}Cs activities with the historical deposition of ^{137}Cs confirms the
 273 validity of the ^{210}Pb -derived ages.

274 Estimated sediment accumulation rate (SAR) increased one order of magnitude
 275 since the beginning of the 19th century, from 0.02 \pm 0.01 cm y^{-1} (MAR of 0.004 \pm

276 0.003 g cm⁻² y⁻¹) in the oldest layers to 0.12 ± 0.02 cm y⁻¹ (MAR of 0.033 ± 0.005 g
277 cm⁻² y⁻¹) in 1970s. After this, the increase in sediment accumulation rates is more
278 pronounced, reaching 0.23 ± 0.02 cm y⁻¹ (MAR of 0.081 ± 0.009 g cm⁻²·y⁻¹) at the
279 surface, which exceeds the background values in a factor of 12.

280 **3.2 Temporal changes in sediment composition**

281 Las Palmas wetland sediment core was composed mainly (> 96%) of silt and clay
282 sized material (Figure 3). On average, bulk sediments contained 2.5 ± 2.4 % of
283 sand (>63 μm), 75 ± 4 % of silt (2 - 63 μm) and 22 ± 5 % of clay (<2 μm). The
284 sediment profile showed a clear decreasing trend of sand content from the bottom
285 to the surface, with a clear peak in 1910. An opposite trend was observed for the
286 clay fraction, with an increase from 20-25% in 1900 to 40% at the beginning of the
287 21th century. TOC content showed values between 2 and 8% (Figure 3b), with a
288 clear peak in ~1940 and decreasing values towards recent times. The range of
289 TOC content in the wetland was similar to those observed in lacustrine sediments
290 from South America (Bertrand et al., 2009; Irurzun et al., 2014), although higher
291 values (between 10 - 40%) have been found in the Quistococha Lake in Peru
292 (Aniceto et al., 2014).

293 Aluminum content ranged from 11% to 16%, increasing from 1930 until a
294 subsurface peak in 1960s (Figure 4). After a short decline, Al content increased
295 again up to maximum values of 16% in recent times. Metal concentrations (Ni, Pb,
296 Cr, Cu and Hg) increased from the basal core sections to the surface (Figure 4).

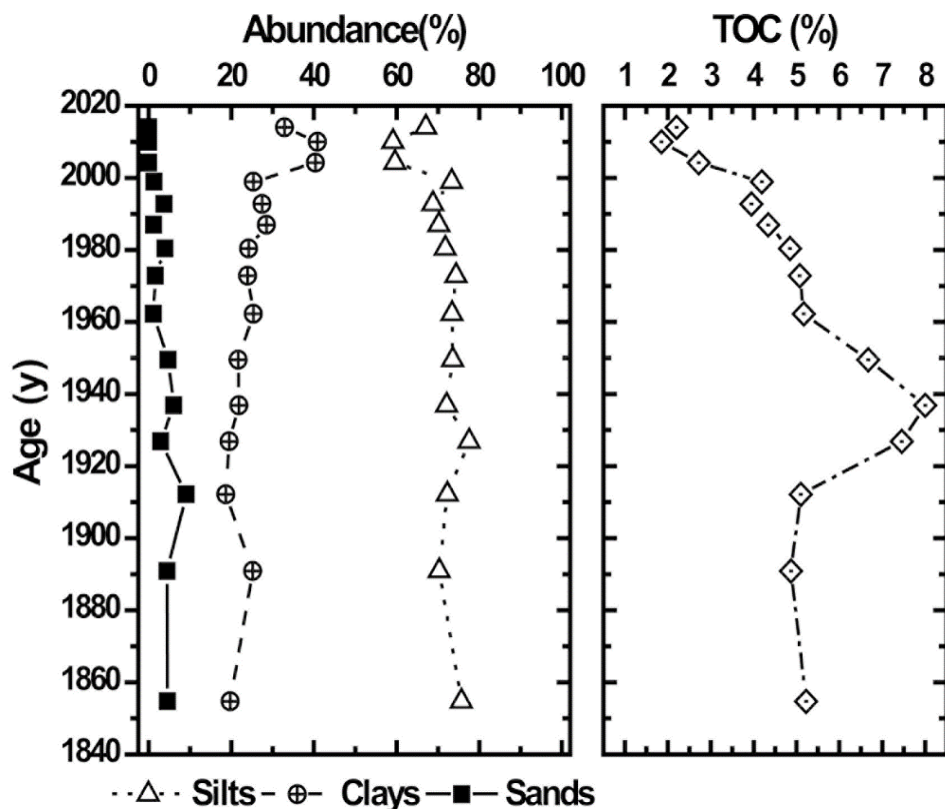


Figure 3. Vertical profile of grain size ((a) Sands, (b) Silts, (c) Clays) and (d) TOC.

297 Surface metal concentrations were higher than background values by a factor of
 298 1.4, 1.7, 1.3, 1.7 for Ni, Pb, Cu, Cr, respectively. Maximum values of Cu ($55 \text{ mg}\cdot\text{kg}^{-1}$)
 299 1) and Pb ($37 \text{ mg}\cdot\text{kg}^{-1}$) were found in sites with low contamination levels (Feria et
 300 al., 2010). Unlike these metals, Zn concentrations were almost constant (around
 301 $160 \text{ mg}\cdot\text{kg}^{-1}$) between 1855 and 1970s. After this, Zn concentrations decreased to
 302 values of $93 \text{ mg}\cdot\text{kg}^{-1}$ at the surface. Trends in Hg concentrations differed from the
 303 rest of metals, with two peaks of maxima concentrations in 1960 and 1980.
 304 Maximum Hg concentrations of $406 \mu\text{g}\cdot\text{kg}^{-1}$ at recent times exceeded two times the
 305 values observed at the beginning of the 19th century. Maximum Hg concentrations
 306 were higher than those reported in sediments of Bajo Cauca - Antioquia $240 \mu\text{g}\cdot\text{kg}^{-1}$
 307 1 (UPME and Universidad de Córdoba, 2015) and sediments of Lake Pillo (20

308 $\mu\text{g}\cdot\text{kg}^{-1}$ to $180 \mu\text{g}\cdot\text{kg}^{-1}$) in Chile (Alvarez et al., 2017). However measured
 309 concentrations were lower than those obtained in sediments of Lake La Señora -
 310 Chile ($734 \mu\text{g}\cdot\text{kg}^{-1}$), where Hg concentrations are associated with the opening of a
 311 chlor-alkali plant of a cellulose industry in the early 1960s (Alvarez et al., 2017).

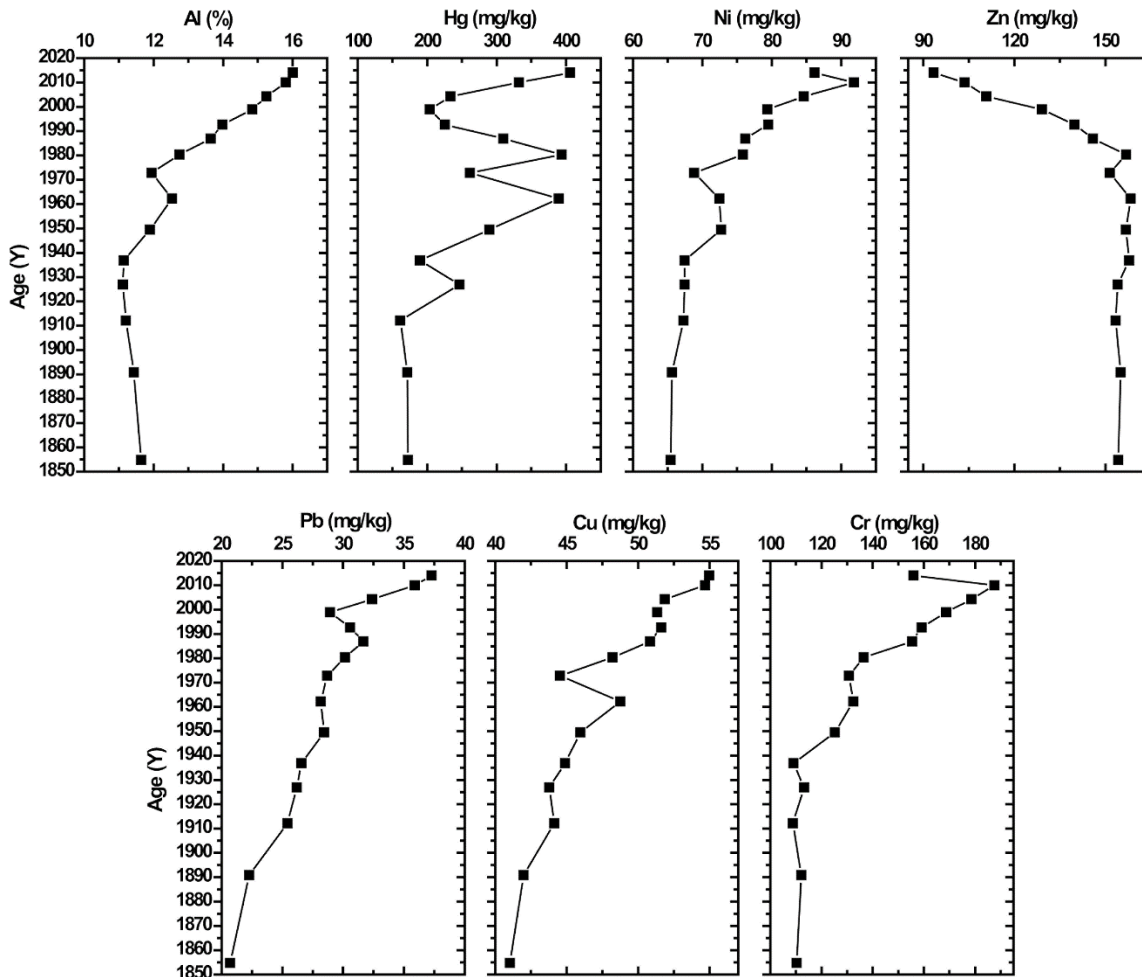


Figure 4. Concentrations profiles of trace metals (Al, Hg, Ni, Zn, Pb, Cu and Cr).

312 Trace metal concentrations in sections older than 1850 are usually taken as pre-
 313 anthropogenic values and considered background or natural levels (Matschullat et
 314 al., 2000; Wei and Wen, 2012). In Las Palmas record, metal concentrations at
 315 these deep layers were within the range of reported background concentrations for
 316 other lakes from South America (Urrutia et al., 2002; Marrugo, 2007; UPME, 2014).

317 However, they were considerably higher than other values observed in other
318 wetland ecosystems in Colombia, for example, Hg background level in Las
319 Palmas was higher than those values reported by Marrugo et al. (2007) in Mojana,
320 likely due to lithological differences between systems. Regarding Hg,
321 concentrations were similar to those determined for Lake La Señoraza (Chile), but
322 considerably higher than in other studies (Urrutia et al., 2002; Feria et al., 2010;
323 Rua et al., 2014; Alvarez et al., 2017). High and variable concentrations during pre-
324 industrial times have been previously observed in other studies that demonstrate
325 that natural concentrations of metals on a scale of thousands of years can be
326 highly changing. This fact may cause a great variability in the metals
327 concentrations in sediments and make difficult to establishing basal values.
328 Background values observed in our core are shown in Table 1, where other
329 background values for other sites of the world are also referenced.

330

332 **3.3 Sediment chemistry: responses to natural and human induced**
333 **changes**

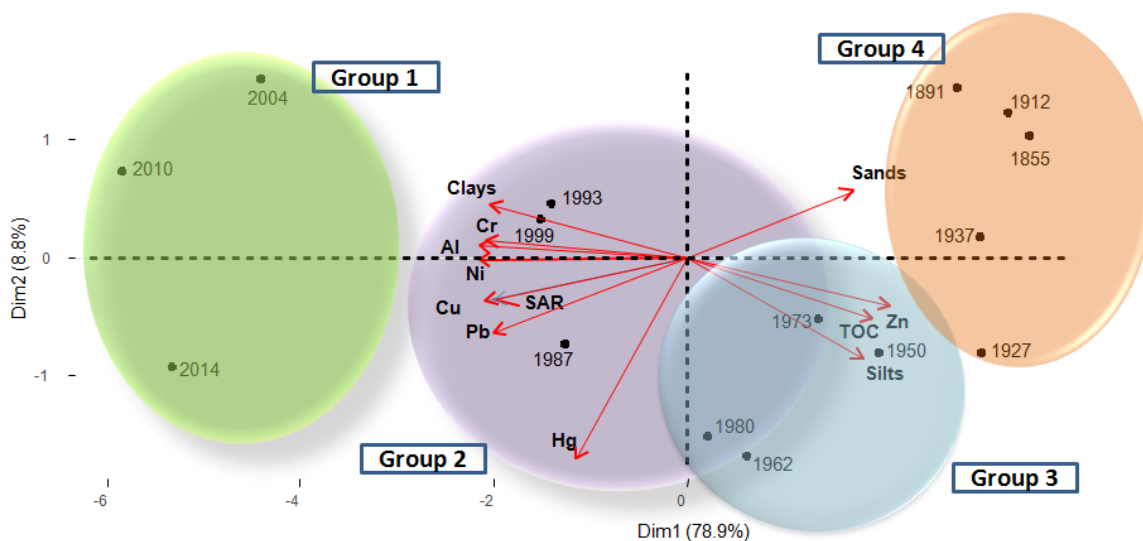
334 In order to understand and delimit the historical evolution of metals concentrations
335 in Las Palmas wetland, a sedimentation temporal framework should be defined
336 considering the ^{210}Pb -derived age model. We used a Principal Component
337 Analysis (PCA) to visualize the temporal variation of the different variables
338 measured in Las Palmas wetland. The result of the PCA applied to metal
339 concentration, granulometry, SAR and TOC distribution together with the age of
340 each sediment section is shown in Figure 4. The PCA showed that Al, Cr, Cu, Ni
341 and Pb were inversely related to TOC, silt and sand content. The analysis also
342 showed that the most important associations occurred between Hg and clay
343 content, and Hg and TOC ($r = 0.39$, $p < 0.05$ and $r = 0.44$, $p < 0.05$, respectively).
344 Unlike the rest of metals, Zn showed a positive relationship with TOC ($r = 0.83$, $p =$
345 0.0001) that indicates the enrichment or deficit of Zn in the presence of organic
346 matter. This is in agreement with previous studies that showed that metals such as
347 Cd and Zn can be absorbed by living plants in areas of high biological activity
348 (Livett et al., 1979; Shotyk, 1996; Espi et al., 1997; Olid et al., 2010). Thus, the
349 presence of macrophytes (*Ludwigia sedoides*, *Paspalum repens* and *Utricularia*
350 *foliosa*) in the wetland might have played a fundamental role in the sequestration of
351 Zn, as well as influence the regulation processes in these ecosystems (Van der
352 Hammen et al., 2008 Kumar and Tripathi, 2008; Maine et al., 2009; Martelo and
353 Lara-Borrero, 2012). The TOC concentration shows a considerable increase
354 between 1910 and 1960, consistent with the exponential population growth,
355 technological changes in the agricultural sector, rural–urban migration and

356 recolonization of lowlands around Cauca river during that period. Total population
357 grew from 6 million to 20 million, while urban population doubled from 30% to 60%.
358 This rapid population growth led to land use changes and also accelerated
359 deforestation processes. The estimated national rate of clearing was around 70000
360 ha per year, with 18000 ha per year corresponding to zones where coffee and
361 other products continued to be grown. The clearing of lowland forests increased
362 with large areas of subhumid and humid forests of the Caribbean, now being
363 cleared at annual rates greater than 2 %. The impact of the cattle industry
364 continued to increase. Of the 28 Mha of cleared land at the end of the period, it is
365 estimated that grazing accounted for more than 80 % (Etter et al., 2008).

366 Finer suspended sediment particles (clays and silt) usually accumulate higher
367 concentrations of heavy metals due to the high content of secondary minerals (Fe,
368 Mn, Al oxides and hydroxides, and carbonates) and organic matter (Hardy and
369 Cornu, 2006). Sand and silt fractions in sediments are largely composed of the
370 primary mineral quartz (e.g., SiO₂), which is a very weak adsorbent for heavy
371 metals. The statistical results of the PCA shows how clays are correlated with Al
372 and heavy metals (Ni, Pb, Cu and Cr) and lesser to extend to Hg. These
373 correlation between clays, Al and metals indicate that the increase of metals in the
374 Las Palmas wetland is due to the presence of higher content of clays
375 (aluminosilicates). Although the correlation of the increase of Al and heavy metals
376 with the increase of the sedimentation rates in the Las Palmas sediment record
377 could be associated with natural processes such as climatic change, the fact that
378 the highest concentrations of Al and metals have been recorded since the 1980s
379 would indicate that such accumulation of metals is due to an increase in

380 anthropogenic activities. In fact, the highest concentrations of metals were
381 recorded since the 1980s.

382 According to the PCA, sediment could be divided into four groups of sediment
383 sections that correspond to different temporal framework (Figure 5). The four group
384 of samples (Group 4) is formed by sections located along the positive axis of the
385 first component and accumulated between 1885 and 1937, characterized by the
386 highest concentrations of sands, silts, TOC and Zn. Sections accumulated between
387 1950 and 1980 are mainly correlated with mercury (Hg) (Group 3), containing the
388 highest Hg concentration. Younger sections of this group 3 accumulated between
389 1950 and 1973, however, are also associated with high concentrations of Zn, TOC
390 and silts. Sections accumulation between 1987 and 1999 showed the strongest
391 correlation between SAR, Clays, Cr, Cu, Ni and Pb (Group 2). Finally, the most
392 recent sections accumulated between 2004 and 2014 (Group 1) are located along
393 the negative axis of the first component, being characterized by the highest values
394 of SAR, Clay, Cr, Cu, Ni and Pb. Both groups (1 and 2) show lower Zn and TOC
395 concentrations with increasing sedimentation rate and clays content.



396

397

Figure 5. PCA applied to a set of sedimentary characteristics.

398

3.4 . Historical evolution of metal fluxes

399

Background metal fluxes showed values of $6.3 \mu\text{g}\cdot\text{m}^{-2}\cdot\text{y}^{-1}$ for Hg and 4.1, 1.5, 2.4

400

and $0.8 \text{mg}\cdot\text{m}^{-2}\cdot\text{y}^{-1}$ for Cr, Cu, Ni and Pb, respectively (Figure 6). All metals had

401

similar trends, with a steady increase since the early 20th century. We observed a

402

first slight increase in metal fluxes from 1910 - 1920 to 1930 - 1940 and a second

403

significant increase from 1970 - 1980 to 2010. For Hg, fluxes increased from $13 \mu\text{g}$

404

$\cdot\text{m}^{-2}\cdot\text{y}^{-1}$ in 1910 to $327 \mu\text{g g}\cdot\text{m}^{-2}\cdot\text{y}^{-1}$ in 2014, equivalent to a 24-fold increase. Cr,

405

Cu, Ni and Pb showed similar fluxes trends, with an increase from 1910 to

406

maximum values in 2010 and a subsequent decrease thereafter. In this period of

407

time, fluxes increased from 9.0, 3.7, 5.6, and $2.1 \text{mg}\cdot\text{m}^{-2}\cdot\text{y}^{-1}$ to 161, 47, 79, and 31

408

$\text{mg}\cdot\text{m}^{-2}\cdot\text{y}^{-1}$ for Cr, Cu, Ni, and Pb, respectively, that represent enrichments up to

409

factor of 13 - 18.

410

Maximum estimated fluxes of Cr, Cu, Ni and Pb are greater than those reported in

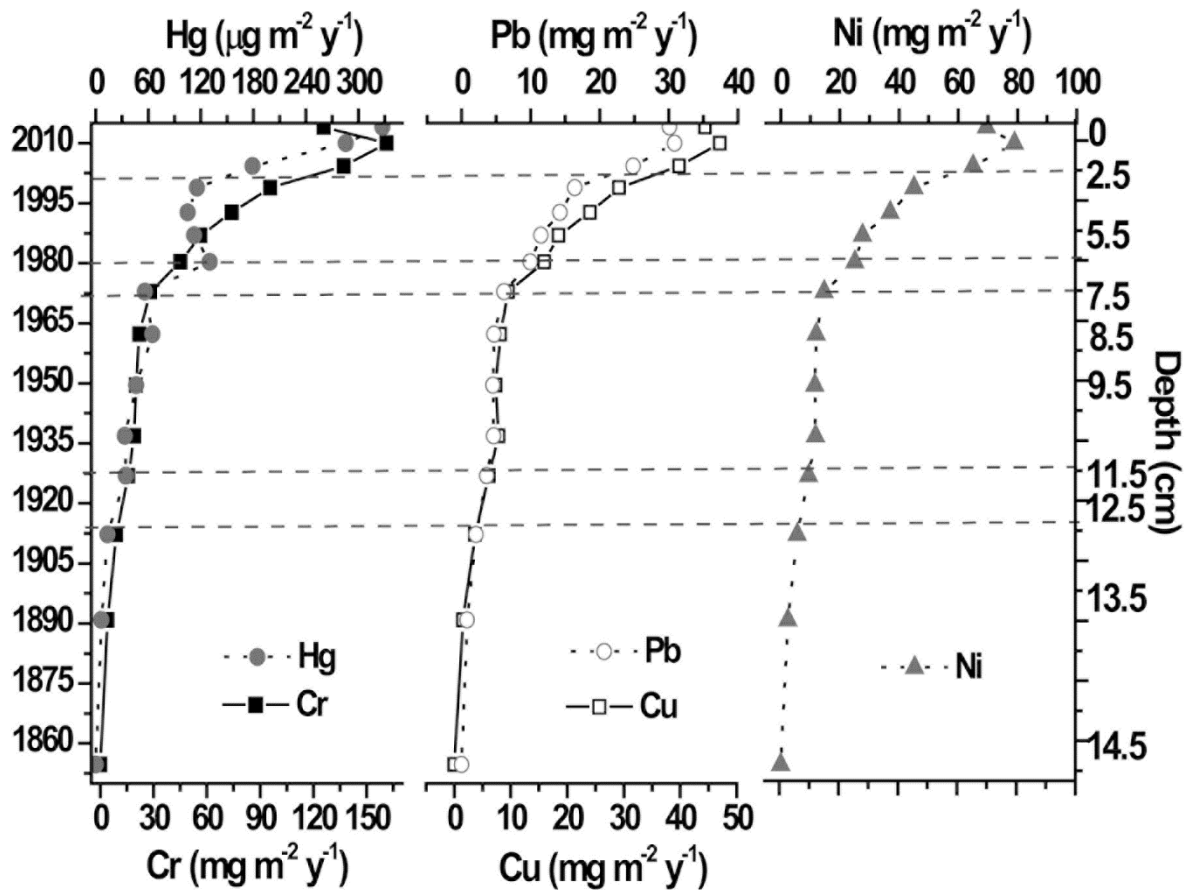
411

other studies performed in other South American lakes. For example, Cooke et al.

412 (2009) reported metals fluxes of $170 - 50 \text{ mg}\cdot\text{m}^{-2}\cdot\text{y}^{-1}$ for Pb, $3.9 \text{ mg}\cdot\text{m}^{-2}\cdot\text{y}^{-1}$ for Hg,
413 $2-10 \text{ mg}\cdot\text{m}^{-2} \text{ y}^{-1}$ for Cu and $1.5 - 3.5 \text{ mg}\cdot\text{m}^{-2}\cdot\text{y}^{-1}$ for Ni, and $5 - 60 \text{ mg}\cdot\text{m}^{-2}\cdot\text{y}^{-1}$ for Zn
414 in Cerro de Pasco (Peruvian Andes). Cooke and Abbott (2008) reported maximum
415 metal fluxes of $30 \text{ mg}\cdot\text{m}^{-2}\cdot\text{y}^{-1}$ for Pb, $10 \text{ mg}\cdot\text{m}^{-2}\cdot\text{y}^{-1}$ for Zn, $4 \text{ mg}\cdot\text{m}^{-2}\cdot\text{y}^{-1}$ for Cu and
416 $1.5 \text{ mg}\cdot\text{m}^{-2}\cdot\text{y}^{-1}$ for Ni, for Chipian lake (Peru) and $200 \text{ mg}\cdot\text{m}^{-2}\cdot\text{y}^{-1}$ for Pb, $60 \text{ mg}\cdot\text{m}^{-2}\cdot\text{y}^{-1}$
417 $2\cdot\text{y}^{-1}$ for Zn, $10 \text{ mg}\cdot\text{m}^{-2}\cdot\text{y}^{-1}$ for Cu and $3.5 \text{ mg}\cdot\text{m}^{-2}\cdot\text{y}^{-1}$ for Ni for Pirhuacocha lake
418 (Peru). Therefore, although the Pb fluxes reported in this study are similar to those
419 presented in other studies, the rest of the metal fluxes are considerably larger.

ECONOMIC ACTIVITIES

Accelerated increase of mining activity
Reactivation of alluvial gold exploitation
Diversification of the economy: crops such as coffee
Intensive exploitation of gold. Expansion of the global economy
Implementation of the amalgam technique with Hg



420

421

Figure 6. Historical metal fluxes calculated for the Las Palmas wetland according to the economic activities.

422 The historical reconstruction of the metal fluxes in Las Palmas wetland reflects the
423 economical evolution of the regional economy mainly related to the agricultural and
424 mining activities (Figure 7). The slight increase in metal fluxes observed from 1910
425 - 1920 to 1930 - 1940 is likely related to the expansion of the world economy
426 during the 1920s and after the First World War, with the consequent demand of
427 gold. During the beginning of the past century, the international prices of gold
428 increased due to of the Great Depression, going from US \$ 18.50 ozt in 1934 to US
429 \$ 35 in 1970. In the late 1930s and early 1940s, there was a wave of colonization
430 in the Bajo Cauca guided by the expectation of a better life based on the gold
431 mining (OECD, 2016). This new settlement process led to changes in vegetation
432 cover as a consequence of changes in land use (e.g. mining, agriculture and wood
433 industry) that probably, increased dramatically the organic matter content in the
434 wetland over several years (Figure 4). However, deforestation and the opening of
435 new ASGM activities increased erosion rates and piles of ground rocks (commonly
436 known as "jales mineros"), which, due to runoff and dust dispersion, reduced TOC
437 content and increased the amount of fine particles entering into Las Palmas
438 wetland. After this period, with the advent of the Second World War, world
439 economies began to recover and world gold exports declined, justifying the almost
440 constant metal fluxes during the 1940 - 1980 period. During this period, the
441 economy of the area diversified based not only on mining, but also on agriculture
442 (e.g. coffee crops, cassava), which used fertilizers such as superphosphate and
443 other phosphates with high concentrations of Cr, Cu, Ni, Pb and Zn (Feria et al.,
444 2010), which probably helped to increase the metal fluxes to the wetland. These
445 deforestation processes established changes in vegetation cover in the wetland

446 area, pasture mosaics (18.4%), mining extraction areas (18.1%) and shrublands
447 (11.4%) (Corantioquia, 2015). However, during this mid-20th century period no
448 significant changes in metals are observed.

449 Between 1970 and 1980, a clear increase in both sedimentation rates and metal
450 fluxes is observed (Figure 6). This is consistent with the reactivation of the mining
451 activities in Colombia and, specifically, with the reactivation of alluvial gold
452 exploitation (AGE) in Antioquia (Betancur-Corredor et al., 2018). This is also in
453 agreement with the fact that at this time, a channel was opened through the
454 wetland to facilitate the access to the area to market the harvested products. The
455 new channel was much shorter, wider and straighter than the natural fluvial
456 connections, which were progressively closed naturally (Corantioquia, 2015). That
457 probably led to the retention of TOC and sands transported to the wetland from the
458 natural connection and reduced the inputs of these materials to Las Palmas, as
459 observed in Figure 4. These changes in the natural dynamics between the river
460 and the wetland reduced significantly the accumulation of silts and increased the
461 accumulation of clays, Al and heavy metals.

462 Finally, the accumulation of heavy metals in recent wetland sediments observed in
463 the late 20th century, is also due to the physical and chemical erosion of the mining
464 waste. These wastes are constituted by crushed polymetallic material containing
465 high specific surface area and high levels of heavy metals such as Pb, Zn, Mn, Cu,
466 Cd, etc., which can be released and subsequently deposited in the bed sediments
467 of the wetland. These changes allowed for foreign investment and exploitation in
468 the area (Duarte, 2012), which considerably intensified mining activities in the Las
469 Palmas wetland. Thus, in recent years, foreign direct investment in mining has

470 almost tripled. This increase in investment implied that Colombia was the largest
471 importer of mercury in Latin America and the Caribbean, with about 130 tons of
472 mercury imported in 2011, 75% of which was used in ASGM activities. That
473 represented the release of between 50 and 100 tons of Hg into the environment
474 (Güiza and Aristizabal, 2013).

475 Mining is not the only activity that causes impacts on wetland ecosystem services.
476 These impacts are more related to the increase of TOC rather than significant
477 increase in metal fluxes as it is observed with mining activities after the 1980s.
478 Changes in land use as crops (coffee, sugar cane, oil palm, coca, and rubber) and
479 cattle ranching also represent a source of metals into the environment. It has been
480 estimated that these activities are responsible for the transformation of 45% of the
481 natural land cover (Etter et al., 2006; Ricaurte et al., 2017) and have led to violent
482 clashes over land ownership and social marginalization, leading to the degradation
483 of large wetland extensions and therefore the increase of metal fluxes. Impacts due
484 to land use change include deforestation due to destruction and loss of vegetation,
485 soil contamination, landscape changes, and soil loss due to disposition of tailings
486 in the vicinity of mining sites and gutters. (Gómez-Rodríguez et al., 2017).

487 This study carried out in Colombia represents a clear example of how the historical
488 evolution of metal fluxes and concentrations recorded in a sediment record reflects
489 the evolution of the regional economy related mainly to agricultural and mining
490 activities. This link is clearly evident between the close relationship between the
491 evolution of the mining economy (% GNP) in Colombia and the flux of Hg recorded
492 in the Las Palmas wetland area (Figure 7). Although there is a clear increase in the
493 Hg flux since 1970, the income that contributes to the gross domestic product due

494 to mining activity has decreased since 2005 due to intermittences in the
495 international price of gold (Güiza and Aristizabal, 2013; Betancur-Corredor et.al.,
496 2018) and not only related to the ASGM activities in Antioquia. Therefore, historical
497 trends in metal concentration in sediments from Las Palmas wetland reflect the
498 degree of socio-economic development in the basin and can be used as a good
499 proxy for evaluating anthropogenic impacts in the area.

500 **Conclusions**

501 This study represents a clear example of how the historical reconstruction of metal
502 fluxes using sediment cores in an impacted wetland reflects the economical
503 evolution of the regional economy mainly related to the agricultural and mining
504 activities in Antioquia (Colombia). Metal fluxes in the wetland evolved according to
505 main three periods of time (Figure 6): from 1910 to 1930; from 1930 to 1970 and
506 from 1970 to 2014. These periods coincide with the economical evolution of
507 Antioquia and worldwide mining activities. Changes in national policies with respect
508 to mining activities implied an increase in the exploitation of natural resources and,
509 consequently, an increase of the release of metals into the environment. However,
510 in order to study the real impact of mining, a more extensive study should be
511 performed around where ASGM activities are carried out.

512 **Acknowledgements**

513 We gratefully acknowledge Joan Manel Bruach for his suggestions and
514 collaboration and the Laboratori de Radioactivitat Ambiental of the Universitat
515 Autònoma de Barcelona for his technical assistance. This project has been funded
516 by the Administrative Department of Science, Technology and Innovation
517 (Colciencias), with the support of the Universidad de Antioquia, Colombia. Jordi

518 Garcia-Orellana wants to thank the support of the Generalitat de Catalunya to
519 MERS (2018 SGR-1588). This work is contributing to the ICTA 'Unit of Excellence'
520 (MinECo, MDM2015-0552).

521 **References**

- 522 Acemoglu, D., García-Jimeno, C., Robinson, J.A., 2012. Finding Eldorado. Slavery
523 and long-run development in Colombia. *J. Comp. Econ.* 40: 534-564.
- 524 Adriano, D.C., 2001. Trace elements in terrestrial environments: Biogeochemistry,
525 bioavailability, and risks of metals. Springer. 411–458.
- 526 Agudelo, D., Molina, F., 2018. Historical record of the mining impact caused by
527 heavy metals in the Las Palmas (Nechí-Antioquia) and San Francisco
528 (Ayapel-Córdoba) wetlands. PhD Thesis.
- 529 Aliyu, A., Majeti, N.V., 2018. Artisanal and small-scale gold mining waste
530 rehabilitation with energy crops and native flora—A case study from Nigeria.
531 *Bio-Geotechnologies for Mine Site Rehabilitation*. Chapter 26: 473-491.
- 532 Alcaldía Municipal de Nechí, “Esquema de Ordenamiento Territorial, Nechí,
533 Antioquia 2000. Sistema de Documentación e Información Municipal,” 2000.
534 Available:<http://www.planesmojana.com/documentos/normatividad/municipa>
535 [I/NECHI/EOT/Documento%20Resumen%20Nechi.pdf](http://www.planesmojana.com/documentos/normatividad/municipa). Accessed
536 September 2019.
- 537 Adler Miserendino, R., Bergquist, B.A., Adler, S.E., Guimarães, J.R.D., Lees,
538 P.S.J., Niquen, W., Velasquez-López, P.C., Veiga, M.M., 2013. Challenges
539 to measuring, monitoring, and addressing the cumulative impacts of
540 artisanal and small-scale gold mining in Ecuador. *Resources Policy*. 38:
541 713-722.

542 Adler Miserendino, R., Guimarães, J.R.D., Schudel, G., Ghosh, S., Godoy, J.M.,
543 Silbergeld, E.K., Lees, P.S.J., Bergquist, B.A., 2017. Mercury pollution in
544 Amapá, Brazil: mercury amalgamation in artisanal and small-scale gold
545 mining or land-cover and land-use changes? *ACS Earth Space Chem* 2,
546 441–450.

547 Álvarez, D., Torrejon, F., Climent, M.J., Garcia-Orellana, J., Araneda, A., Urrutia,
548 R., 2017. Historical anthropogenic mercury in two lakes of central Chile:
549 Comparison between an urban and rural lake. *Environ Sci Pollut Res.* 25(5):
550 4596-4606.

551 Aniceto, K., Moreira-Turcq, P., Cordeiro, R.C., Fraizy, P., Quintana, I., Turcq, B.,
552 2014. Holocene paleohydrology of Quistococha Lake (Peru) in the upper
553 Amazon Basin: Influence on carbon accumulation. *Palaeogeography,*
554 *Palaeoclimatology, Palaeoecology.* 415: 165-174.

555 Appleby, P., Oldfield, F., 1992. Applications of lead-210 to sedimentation studies,
556 Uranium-series disequilibrium: applications to earth, marine, and
557 environmental sciences. 2. ed.

558 Appleby, P. 2001. Chronostratigraphic techniques in recent sediments, Tracking
559 environmental change using lake sediments. Springer. 171-203.

560 Arias-Ortiz, A., Masqué, P., Garcia-Orellana, J., Serrano O., Mazarrasa I., Marbà
561 N., Lovelock C.E., Lavery P.S., and Duarte C.M., 2018. Reviews and
562 syntheses: ²¹⁰Pb-derived sediment and carbon accumulation rates in
563 vegetated coastal ecosystems – setting the record straight. *Biogeosciences.*
564 15: 6791–6818.

565 Balzino, M., Seccatore, J., Marin, T., De Tomi, G., Veiga, M.M., 2015. Gold losses
566 and mercury recovery in artisanal gold mining on the Madeira River, Brazil.
567 J. Clean. Prod. 102: 370–377.

568 Bertrand, S., Sterken, M., Vargas-Ramirez, L., De Batist, M., Vyverman, W.,
569 Lepoint, G., Fagel, N., 2009. Bulk organic geochemistry of sediments from
570 Puyehue Lake and its watershed (Chile, 40°S): Implications for
571 paleoenvironmental reconstructions. *Palaeogeography, Palaeoclimatology,*
572 *Palaeoecology.* 294: 56-71.

573 Betancur-Corredor, B., Loaiza-Usuga J.C., Denich M., Borgemeister, C., 2018.
574 Gold mining as a potential driver of development in Colombia: Challenges
575 and opportunities. *Journal of Cleaner Production* 199: 538-553.

576 Betancur, T., Mejia, O., and Palacio C., 2009. Modelo hidrogeológico conceptual
577 del Bajo Cauca antioqueño: un sistema acuífero tropical, *Rev. Fac. Ing.*
578 *Univ. Ant., no. 48,* pp. 107-118.

579 Birch, G.F., 2017. Determination of sediment metal background concentrations and
580 enrichment in marine environments – A critical review. *Science of the Total*
581 *Environment.* 580: 813–831.

582 Camizuli, E., Scheifer R., Garnier S., Monna F., Losno R., Gourault C., Hamm G.,
583 Lachiche C., Delivet G., Chateau C., Alibert P.,. 2018. Trace metals from
584 historical mining sites and past metallurgical activity remain bioavailable to
585 wildlife today. *Scientific Reports* 8: 3436.

586 CEDEX, 1994. Recomendaciones Para la Gestión Del Material Dragado en
587 Puertos Españoles. Ministerio de Obras Públicas, Transportes y Medio
588 Ambiente, Madrid. Available: <http://www.puertos.es/es->

589 es/BibliotecaV2/CEDA-Specific-Suggestions-Spanish-DM-guidelines-draft-
590 directrices2015_tcm7-325119-marked.pdf. Accessed September 2019.

591 Chapman P.M., 2007. Determining when contamination is pollution — Weight of
592 evidence determinations for sediments and effluents. *Environment*
593 *International*. 33: 492-501.

594 Chen, C.F., Ju, Y.R., Chen, C.W., Dong, C.D., 2016. Vertical profile, contamination
595 assessment, and source apportionment of heavy metals in sediment cores
596 of Kaohsiung Harbor, Taiwan. *Chemosphere*. 165: 67-79.

597 Cooke, C. and Abbott, M., 2008. A paleolimnological perspective on industrial-era
598 metal pollution in the central Andes, Peru. *The Science of the total*
599 *environment*. 393. 262-72.

600 Cooke, C.A., Wolfe, A.P., and Hobbs, W.O., 2009. Lake-sediment geochemistry
601 reveals 1400 years of evolving extractive metallurgy at Cerro de Pasco,
602 Peruvian Andes: *Geology*. 37: 1019–1022.

603 Cordy, P., Veiga, M.M., Salih, I., Al-Saadi, S., Console, S., Garcia, O., Mesa, L.A.,
604 Velasquez-L opez, P.C., Roeser, M., 2011. Mercury contamination from
605 artisanal gold mining in Antioquia, Colombia: the world's highest per capita
606 mercury pollution. *Sci. Total Environ*. 410-411, 154-160.

607 Corantioquia, 2015. Sustento para la declaratoria de un área protegida pública en
608 los complejos cenagosos el sapo y hoyo grande, municipio de Nechí,
609 Antioquia. Available:
610 [http://www.corantioquia.gov.co/ciadoc/FAUNA/AIRNR_CV_1412_120_2014.](http://www.corantioquia.gov.co/ciadoc/FAUNA/AIRNR_CV_1412_120_2014.pdf)
611 pdf. Accessed September 2019

612 Daga, R., Ribeiro-Guevara, S., Pavlin, M., Rizzo, A., Lojen, S., Vreča, P., Horvat,
613 M., Arribére, M., 2016. Historical records of mercury in southern latitudes
614 over 1600 years: Lake Futalaufquen, Northern Patagonia. *Sci Total Environ.*
615 553: 541–550.

616 De Paula, F.F., Marins, R.V., De Lacerda, L.D., Aguiar, J.E., Farias Peres, T.,
617 2015. Background values for evaluation of heavy metal contamination in
618 sediments in the Parnaíba River Delta estuary, NE/Brazil, *Marine Pollution*
619 *Bulletin.* 91 (2): 424-428.

620 Devesa-Rey, R., Diaz-Fierros, F., Barral, M.T., 2011. Assessment of enrichment
621 factors and grain size influence on the metal distribution in riverbed
622 sediments (Anllóns River, NW Spain). *Environ. Monit. Assess.* 179: 371–
623 388.

624 Diringer, S., Berky, A., Pan, W.K.Y., Hsu-kim, H., 2015. River transport of mercury
625 from artisanal and small-scale gold mining and risks for dietary mercury
626 exposure in Madre de Dios, Peru. *Environ. Sci. Processes Impacts* 478–
627 487.

628 Duarte, C., 2012. Gobernabilidad minera: cronologías legislativas del subsuelo en
629 Colombia, Centro de Pensamiento RAIZAL. Available:
630 [https://governabilidadminera.files.wordpress.com/2012/01/governabilidad-](https://governabilidadminera.files.wordpress.com/2012/01/governabilidad-minera-cronologicc81as-legislativas-del-subsuelo-en-colombia.pdf)
631 [minera-cronologicc81as-legislativas-del-subsuelo-en-colombia.pdf](https://governabilidadminera.files.wordpress.com/2012/01/governabilidad-minera-cronologicc81as-legislativas-del-subsuelo-en-colombia.pdf).
632 Accessed September 2019.

633 Espi, E., Boutron, C.F., Hong, S., Pourchet, M., Ferrari, C., Shotyk, W., and
634 Charlet, L., 1997. Changing concentrations of Cu, Zn, Cd and Pb in a high

635 altitude peat bog from Bolivia during the past three centuries. *Water, Air and*
636 *Soil Pollut.* 100:289-296.

637 Etter, A., McAlpine, C., Phinn, S., Pullar, D., Possingham, H., 2006. Unplanned
638 land clearing of Colombian rainforests: spreading like disease? *Landsc.*
639 *Urban Plan.* 77, 240–254.

640 Etter, A., McAlpine, C., Phinn, S., Possingham, H., 2008. Historical patterns and
641 drivers of landscape change in Colombia since 1500: A regionalized spatial
642 approach. *Annals of the Association of American Geographers*, 98(1): 2–23.

643 Feria, J.J., Marrugo, J.L., González, H., 2009. Heavy metals in Sinú river,
644 department of Córdoba, Colombia, South America. En: *Revista*
645 *Facultad de Ingeniería Universidad de Antioquia* 55 (35-44) 2422-2844.

646 Flynn, W. 1968. The determination of low levels of polonium-210 in environmental
647 materials: *Analytica chimica acta*, 43: 221-227.

648 Gan, H., Lin, J., Liang, K., Xia, Z., 2013. Selected trace metals (As, Cd and Hg)
649 distribution and contamination in the coastal wetland sediment of the
650 northern Beibu Gulf, South China Sea. *Marine Pollution Bulletin.* 66 (1–2):
651 252-258.

652 Garcia, O., Veiga, M.M., Cordy, P., Suescún, O.E., Molina, J.M., Roeser, M., 2015.
653 Artisanal gold mining in Antioquia, Colombia: a successful case of mercury
654 reduction. *J. Clean. Prod.* 90, 244-252.

655 Garcia-Orellana, J., Cañas, L., Masqué, P., Obrador, B., Olid, C., Pretus, J., 2011.
656 Chronological reconstruction of metal contamination in the Port of Maó
657 (Minorca, Spain). *Marine Pollution Bulletin.* 62: 1632-1640.

658 Gerson, J.R., Driscoll, C.T., Hsu-Kim, H., Bernhardt, E.S., 2018. Senegalese
659 artisanal gold mining leads to elevated total mercury and methylmercury
660 concentrations in soils, sediments, and rivers. *Elem Sci Anth.* 6: 11.

661 Gómez-Rodríguez, M.E., Molina-Pérez, F.J., Agudelo-Echavarría, D.M., Cañón-
662 Barriga, J.E., Vélez-Macías, F., 2017. Changes in soil cover in Nechí,
663 Antioquia: An approach to the environmental impact of mining, 1986-2010.
664 *Revista Facultad de Ingeniería (Rev. Fac. Ing.)*. 26 (45): 149-163.

665 Grimaldi, C., Grimaldi, M., Guedron, S., 2008. Mercury distribution in tropical soil
666 profiles related to origin of mercury and soil processes. *Sci. Total Environ.*
667 40: 121–129.

668 Gu, Y.G., Lin, Q., Yu, Z.L., Wang, X.N., Ke, C.L., Ning, J.J., 2015. Speciation and
669 risk of heavy metals in sediments and human health implications of heavy
670 metals in edible nekton in Beibu Gulf, China: a case study of Qinzhou Bay.
671 *Mar. Pollut. Bull.* 101 (2): 852–859.

672 Güiza, L., Aristizabal, J.D., 2013. Mercury and gold mining in Colombia: a failed
673 state. *Univ. Sci.* 18 (1): 33-49.

674 Hamilton, T.F., Smith, J.D., 1986. Improved alpha energy resolution for the
675 determination of polonium isotopes by alpha-spectrometry: *International*
676 *Journal of Radiation Applications and Instrumentation. Part A. Applied*
677 *Radiation and Isotopes*, 37 (7): 628-630.

678 Hardy, M., Cornu, S., 2006. Location of natural trace elements in silty soils using
679 particle-size fractionation. *Geoderma.* 133: 295–308.

680 Hilson, G., 2016. Farming, small-scale mining and rural livelihoods in sub-Saharan
681 Africa: a critical overview. *Extr. Ind. Soc.* 3 (2): 547–563.

682 Ho, H.H., Swennen, R., Van Damme, A., 2010. Distribution and contamination
683 status of heavy metals in estuarine sediments near Cua Ong Harbor, Ha
684 Long Bay, Vietnam. *Geol. Belgica* 13 (1), 37–47.

685 Irurzun, M.A., Gogorza, C.S.G., Sinito, A.M., Chaparro, M.A.E, Prieto, A.R.,
686 Laprida, C., Lirio, J.M., Navas, A.M., Nuñez, H., 2014. A high-resolution
687 palaeoclimate record for the last 4800 years from lake la Brava, SE pampas
688 plains, Argentina. *Geofísica Internacional*. 53(4): 365-383.

689 ISO B, 2009. 13320: 2009 Particle size analysis-laser diffraction methods.

690 ISO N, 1998. 14235, 1998: Soil quality [Determination of organic carbon by
691 sulfochromic oxidation. TC 190/SC 3.

692 Kahhat, R., Parodi, E., Larrea-Gallegos, G., Mesta, C., Vázquez-Rowe, I., 2019.
693 Environmental impacts of the life cycle of alluvial gold mining in the Peruvian
694 Amazon rainforest. *Science of The Total Environment*. 662: 940-951.

695 Kang, B., Wang, D., Du, S., 2017. Source Identification and Degradation Pathway
696 of Multiple Persistent Organic Pollutants in Groundwater at an Abandoned
697 Chemical Site in Hebei, China. 9: 1–7.

698 Kumar V.M., Tripathi B.D., 2008. Concurrent removal and accumulation of heavy
699 metals by the three aquatic macrophytes. *Bioresource Technology*. 99 (15):
700 7091-7097.

701 Lar, U.A., Ngozi-Chika, C.S., Tsuwang, K.D., 2015. Environmental health impact of
702 potentially harmful element discharges from mining operations in Nigeria. In
703 Proc Closing Workshop IGCP/SIDA. 75–79. (Prague, Czech Republic).

704 Livett, E.A., Lee, E.A., Tallis, T.H., 1979. Lead, zinc and copper analyses of British
705 blanket peats. *J. Ecol.* 67, 865–891.

706 Long, E.R., MacDonald, D.D., Smith, S.L., Calder, F.D., 1995. Incidence of
707 adverse biological effects within ranges of chemical concentrations in
708 marine and estuarine sediments. *J. Environ. Manage.* 19: 81–97.

709 Loring, D., Rantala, R., 1992. Manual for the geochemical analyses of marine
710 sediments and suspended particulate matter: *Earth-Science Reviews*, 32
711 (4): 235-283.

712 MacDonald, D.D., Ingersoll, C.G., Berger, T.A., 2000. Development and
713 evaluation of consensus-based sediment quality guidelines for fresh-water
714 ecosystems. *Arch. Environ. Contam. Toxicol.* 39, 20–31.

715 Maine, M.A., Suñe, N., Hadad, H., Sánchez, G., Bonetto, C., 2009. Influence of
716 vegetation on the removal of heavy metals and nutrients in a constructed
717 wetland, *Journal of Environmental Management.* 90 (1): 355-363.

718 Manoj, M.C., Thakur B., Raj Uddandam P., Prasad V., 2018. Assessment of
719 metal contamination in the sediments of Vembanad wetland system, from
720 the urban city of southwest India. *Environmental Nanotechnology,
721 Monitoring & Management.* 10: 238-252.

722 Marshall, B.G., Veiga, M.M., Kaplan, R.J., Adler Miserendino, R., Schudel, G.,
723 Bergquist, B., Guimarães, J.R., Sobral, L.G.S., Gonzalez-Mueller, C.,
724 2018. Evidence of transboundary mercury and other pollutants in the
725 Puyango-Tumbes River basin, Ecuador-Peru. *Environmental Science:
726 Processes & Impacts* 20, 632–641.

727 Marrugo-Negrete J., Pinedo-Hernández J., Díez S., 2017. Assessment of heavy
728 metal pollution, spatial distribution and origin in agricultural soils along the
729 Sinú River Basin, Colombia. *Environmental Research* 154: 380–388.

730 Moreno-Brush, M., Rydberg, J., Gamboa, N., Storch, I., Biester, H., 2016. Is
731 mercury from small-scale gold mining prevalent in the southeastern
732 Peruvian Amazon? *Environ. Pollut.* 218, 150–159.

733 Martelo, J., Lara-Borrero, J.A., 2012. Floating macrophytes on the wastewater
734 treatment: a state of the art review. *Ingeniería y Ciencia, ing. cienc.* 8 (15):
735 221–243.

736 Matschullat, J.; Ottenstein, R.; Reimann, C., 2000. Geochemical background—Can
737 we calculate it?. *Environ. Geol.* 39: 990–1000.

738 Mora, A.; Jumbo-Flores, D.; González-Merizalde, M.; Bermeo-Flores, S.;
739 Alvarez-Figueroa, P.; Mahlkecht, J.; Hernández-Antonio, A., 2018. Heavy
740 Metal Enrichment Factors in Fluvial Sediments of an Amazonian Basin
741 Impacted by Gold Mining. [Bulletin of Environmental Contamination and](#)
742 [Toxicology](#) vol.102, p. 210–217.

743 Niane, B., Moritz, R., Guédron, S., Ngom, P.M., Pfeifer, H.R., Mall, I., Poté, J.,
744 2014. Effect of recent artisanal small-scale gold mining on the contamination
745 of surface river sediment: case of Gambia River, Kedougou region,
746 southeastern Senegal. *J. Geochem. Explor.* 144: 517–527.

747 Olid, C., Garcia-Orellana, J., Martínez-Cortizas, A., Masqué, P., Peiteado-Varela,
748 E., Sanchez-Cabeza, A. 2010. Multiple site study of recent atmospheric
749 metal (Pb, Zn and Cu) deposition in the NW Iberian Peninsula using peat
750 cores. *Science of the Total Environment.* 408: 5540-5549.

751 Olid, C., 2011. Evaluating the reliability of ²¹⁰Pb-dated peat bog cores to
752 reconstruct atmospheric metal deposition in NW Spain. Thesis PhD.

753 Departament de Física. Facultat de Ciències. Universitat Autònoma de
754 Barcelona.

755 Palacios-Torres, Y., Caballero-Gallardo, K., Olivero-Verdel J., 2018. Mercury
756 pollution by gold mining in a global biodiversity hotspot, the Choco
757 biogeographic region, Colombia. *Chemosphere* 193: 421-430.

758 Paulson, A., Norton, D., 2008. Mercury sedimentation in lakes in western Whatcom
759 County, Washington, USA and its relation to local industrial and municipal
760 atmospheric sources. *Water Air Soil Pollut.* 189:5–19.

761 Pennington, W., Cambray R.S., and Fisher E.M.. 1973. Observations on lake
762 sediments using fallout ¹³⁷CS as a tracer. *Nature (London)* 242:324-326.

763 Puig, P., and Palanques, A., 1998. Temporal variability and composition of settling
764 particle fluxes on the Barcelona continental margin (Northwestern
765 Mediterranean). *Journal of marine research.* 56(3): 639-54.

766 Rencher, A., 2002. *Methods of Multivariate Analysis*. Second Edition. John Wiley &
767 Sons, Inc.

768 Ricaurte, L.F., Olaya-Rodríguez, M.H., Cepeda-Valencia, J., Lara, D., Arroyave-
769 Suárez, J., Max Finlayson, C., Palomo, I., 2017. Future impacts of drivers of
770 change on wetland ecosystem services in Colombia. *Global Environmental*
771 *Change* 44: 158–169.

772 Rúa, A., Liebezeit, G., Palacio-Baena, J., 2014. Mercury colonial footprint in Darién
773 Gulf sediments, Colombia. *Environmental Earth Sciences.* 71 (4): 1781-
774 1789.

775 Rungwa, S., Arpa, G., Sakulas, H., Harakuwe, A., Tim, D., 2013. Phytoremediation
776 an eco-friendly and sustainable method of heavy metal removal from closed

777 mine environments in Papua New Guinea. *Proced. Earth and Planet. Sci.* 6,
778 269-277.

779 Sanchez-Cabeza, J. A., Masque P., Ani-Ragolta I., 1998. ^{210}Pb and ^{210}Po
780 analysis in sediments and soils by microwave acid digestion. *Journal of*
781 *Radioanalytical and Nuclear Chemistry* 227 (1-2) 19-22.

782 Sanchez-Cabeza J. A., Díaz-Asencio M., Ruiz-Fernandez A. C. 2012.
783 Radiocronología de sedimentos costeros utilizando ^{210}Pb : Modelos,
784 validación y aplicaciones. Organismo internacional de energía atómica,
785 Viena.

786 Sang-Han, L., Pavel, P., Povinec, E.W., Mai, K., Pham Gi-Hoon, H., Chang-Su, C.,
787 Suk-Hyun, K., Hee-Jun, L., 2005. Distribution and inventories of ^{90}Sr ,
788 ^{137}Cs , ^{241}Am and Pu isotopes in sediments of the Northwest Pacific
789 Ocean. *Marine Geology*. 216 (4): 249-263.

790 Shotyk, W., Cheburkin, A.K., Appleby, P.G., Fankhauser, A., and Kramers, J.D.,
791 1996. Two thousand years of atmospheric arsenic, antimony, and lead
792 deposition recorded in an ombrotrophic peat bog profile, Jura Mountains,
793 Switzerland. *Earth Plan et Sci. Lett.* 145: E1-E7.

794 Silva-Filho, E.V., Machado, W., Oliveira, R.R., Sella, S.M., Lacerda, L.D., 2006.
795 Mercury deposition through litterfall in an Atlantic Forest at Ilha Grande,
796 Southeast Brazil. *Chemosphere*. 65: 2477–2484.

797 Singh, J., and Kalamdhad, A., 2011. Effects of Heavy Metals on Soil, Plants,
798 Human Health and Aquatic Life. *International Journal of Research in*
799 *Chemistry and Environment*. 1 (2): 15-21.

800 Smith, J.N., 2001. Why should we believe ^{210}Pb sediment geochronologies?.

801 Journal of Environmental Radioactivity. 55: 121-123.

802 Stupar, Y., Schäfer, J., García, M., Schmidt, S., Piovano, E., Blanc, G., Huneau, F.,

803 Le Coustumer, P., 2014. Historical mercury trends recorded in sediments

804 from the Laguna de la Plata, Córdoba, Argentina. Chem Erde. 74(3):353–

805 363.

806 Telmer, K.H., Veiga, M.M., 2009. World Emissions of Mercury From Artisanal and

807 Small Scale Gold Mining. 131–172.

808 Unidad de Planeación Minero Energética-UPME, 2014. Estudio de la cadena del

809 mercurio en Colombia con énfasis en la actividad minera de oro. Ministerio

810 de Minas y Energía- Unidad de Planeación Minero Energética (UPME) y

811 Universidad de Córdoba. Bogotá. Available:

812 <https://bdigital.upme.gov.co/bitstream/001/1315/4/v.2.pdf>. Accessed

813 September 2019.

814 United Nations Environment Programme-UNEP, 2018. Global Mercury

815 Assessment 2018: Sources, Emissions, Releases and Environmental

816 Transport. UNEP Chemicals Branch, Geneva, Switzerland.

817 UNODC y Ministerio de Justicia, 2018. Colombia: Explotación de oro de aluvión

818 Evidencias a partir de percepción remota. Programa de las Naciones

819 Unidas para el Desarrollo-PNUD y Fondo para el Medio Ambiente Mundial.

820 UPME y Universidad de Córdoba, 2015. Incidencia real De La minería del Carbón,

821 del Oro y del uso del Mercurio en la calidad ambiental con énfasis Especial

822 en el Recurso Hídrico - Diseño De Herramientas Para La Planeación

823 Sectorial. Ministerio de Minas y Energía. Bogotá - Colombia. p. 663.

824 Available: <http://www1.upme.gov.co/simco/Cifras->
825 [Sectoriales/EstudiosPublicaciones/Incidencia_real_de_la_mineria_sobre_el](http://www1.upme.gov.co/simco/Cifras-Sectoriales/EstudiosPublicaciones/Incidencia_real_de_la_mineria_sobre_el_recurso_hidrico.pdf)
826 [_recurso_hidrico.pdf](http://www1.upme.gov.co/simco/Cifras-Sectoriales/EstudiosPublicaciones/Incidencia_real_de_la_mineria_sobre_el_recurso_hidrico.pdf). Accessed September 2019.

827 Urrutia, R., Yevenes, M., Barra, R., 2002. Determinación de los niveles basales de
828 metales traza en sedimentos de tres lagos andinos de Chile: lagos
829 Chungará, Laja y Castor. Boletín de la Sociedad Chilena de Química. 47(4).

830 Van der Hammen, T., Stiles, F.G., Rosselli, L., Chisacá-Hurtado, M.L., Camargo
831 Ponce de León, G., Guillot Monroy, G., Useche Salvador, Y., Rivera Ospina,
832 D., 2008. Protocolo de recuperación y rehabilitación ecológica de
833 humedales en centros urbanos. Secretaría Distrital de Ambiente, Bogotá,
834 300p.

835 Wei, C.; Wen, H. Geochemical baselines of heavy metals in the sediments of two
836 large freshwater lakes in China: Implications for contamination character
837 and history. Environ. Geochem. Health 2012, 34, 737–748.

838 World health statistics (WHO). 2013. World Health Organization

839 Zapata, G., Bermudez, J.G., Rodríguez, G., Arango, M.I., 2013. Cartografía
840 Geológica de la Plancha 83 Nechí (Departamento de Antioquia). Ministerio
841 de Minas y Energía-Servicio Geológico Colombiano. Bogotá.

842 Zhu, H., Bing, H., Wu, Y., Zhou, J., Sun, H., Wang, J., Wang, X., 2019. The spatial
843 and vertical distribution of heavy metal contamination in sediments of the
844 Three Gorges Reservoir determined by anti-seasonal flow regulation.
845 Science of The Total Environment. 664: 79-88.

846